Infrared Physics and Technology 105 (2020) 103208

Contents lists available at ScienceDirect

Infrared Physics & Technology

journal homepage: www.elsevier.com/locate/infrared

Self-Q-switched operation in Tm:YAG crystal and passively Q-switched operation using GaSe saturable absorber

W. Zhang*, H.L. Bai, L.P. Guo, M.X. Li*

School of Science, Changchun University of Science and Technology, Changchun 130022, China

ARTICLE INFO

Keywords:
Self-Q-switched
Tm:YAG crystal
GaSe saturable absorber
Passively Q-switched

ABSTRACT

In this paper, we investigated the self-Q-switched (SQS) operation in Tm:YAG crystal. The diode-pumped SQS Tm:YAG laser was operated at a central wavelength of 2006 nm. With the pump power of 4.4 W, we got two sets of data: (1) the optical conversion efficiency of the SQS operation with output coupler (OC) of 10% was 12.50%, and the corresponding output power was 0.55 W; (2) the optical conversion efficiency of the SQS operation with OC of 15% was 19.77%, and the corresponding output power was 0.87 W. Thus, Tm:YAG crystal could be widely used in SQS lasers. In addition, GaSe saturable absorbers (SAs) with broadband nonlinear saturable absorption properties were fabricated and employed as SAs for passively Q-switched Tm:YAG lasers. Attributing to the weak evanescent field and long interaction length, GaSe SAs could work at high-power regime and wide-wavelength range. In summary, GaSe is a good 2D SA material in wide-wavelength range.

1. Introduction

In recent years, passively Q-switched lasers were of great significance on many respects such as scientific research, medical application, material processing, range finding, remote sensing and nonlinear frequency conversion [1]. Compared with passively Q-switched lasers, SQS operation could avoid the complex structure and the insert loss of Q-switchers. Thus, the SQS crystals have become a research focus among native and foreign researchers. SQS operation firstly reported in ruby lasers by Freund [2], and SQS is a simple Q-switched operation without any other modulation elements inside the laser cavity. In recent years, many crystals were used in SQS lasers [3–9].

Transition-metal dichalcogenides (TMD) are highly anisotropic layered materials. With excellent physical–chemical properties, they could instead complement graphene and other semiconductors in many fields [10–13]. The typical TMD materials are tungsten disulfide (WS_2), molybdenium disulfide (MoS_2) and so on. Gallium selenide (GaSe) is a p-type semiconductor with high-resistivity layered structure [14,15]. The bandgap energy (2.11 eV) of GaSe is closely to direct bandgap, which makes electrons easily to transfer with smaller thermal energy [16,17]. With wide optical transparency from visible to far-infrared, high birefringence characteristics, high thermal stability and high laser threshold damage, GaSe could be widely used in many optical systems. Moreover, GaSe was employed in fields of transistors, photo detectors, nanophotonics devices, second harmonic generation nonlinear optical materials and THz emitters.

In this paper, we investigated the self-Q-switched (SQS) operation in Tm:YAG crystal. The diode-pumped SQS Tm:YAG laser was operated at a central wavelength of 2006 nm. With the pump power of 4.4 W, we got two sets of data: (1) the optical conversion efficiency of the SQS operation with output coupler (OC) of 10% was 12.50%, and the corresponding output power was 0.55 W; (2) the optical conversion efficiency of the SQS operation with OC of 15% was 19.77%, and the corresponding output power was 0.87 W. Thus, Tm:YAG crystal could be widely used in SQS lasers. In addition, GaSe saturable absorber (SA) was fabricated by liquid phase stripping method. The Raman spectrometer, atomic force microscope (AFM) and nonlinear absorption spectrum were used to characterize the molecular bond, morphology, layer number and saturable absorption properties of GaSe SA. In summary, GaSe is a good 2D SA material in wide-wavelength range.

2. Experiential setup

Fig. 1 shows the experimental setup of the SQS Tm:YAG laser. The pump light source was a fiber-coupled diode-laser with the central wavelength of 792 nm. Through focusing optics with numerical aperture of 0.22, the pump light was focused into the laser crystal. The Tm:YAG crystal had a dimensions of 3 mm × 3 mm × 5 mm with Tm concentration of 2 at.%. The input mirror M_1 was flat mirror with HR (high-reflection)-coated at 2 μm and HT (high-transmission)-coated at

* Corresponding author.
E-mail addresses: a5371863@163.com (W. Zhang), 15754374309@163.com (M.X. Li).

https://doi.org/10.1016/j.infrared.2020.103208
Received 30 November 2019; Received in revised form 15 January 2020; Accepted 18 January 2020
Available online 22 January 2020
1350-4495/

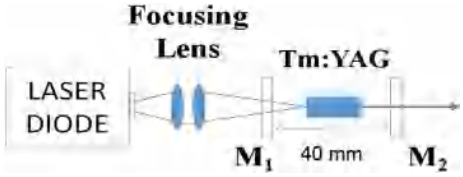

Fig. 1. Experiential setup of the SQS Tm:YAG laser.

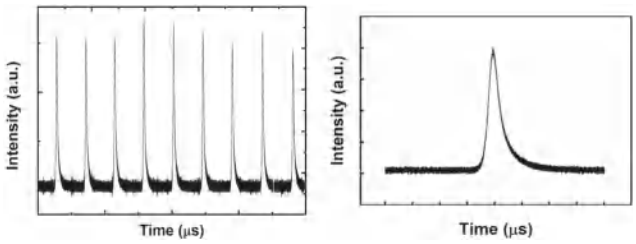

(a) Multiple pulse trains (50μs/div) (b) One typical pulse profile (5μs/div)

Fig. 2. The pulse train of the SQS Tm:YAG laser with OC of 10%.

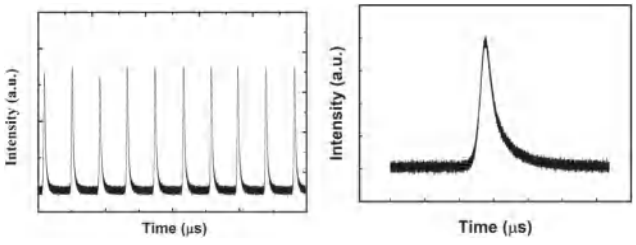

(a) Multiple pulse trains (50μs/div) (b) One typical pulse profile (5μs/div)

Fig. 3. The pulse train of the SQS Tm:YAG laser with OC of 15%.

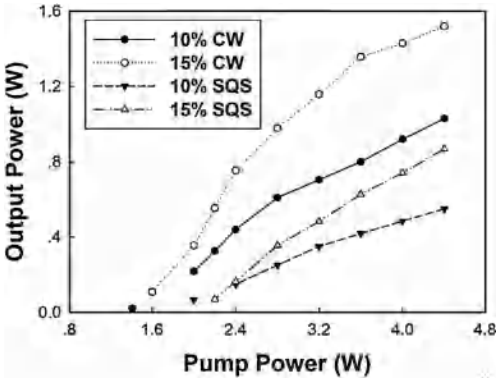

Fig. 4. The output power versus the incident pump power under CW and SQS operations.

792 nm. The crystal with cooling temperature at 20 ˚C is used. The OC mirror M_2 was a flat mirror with transmission of 10% and 15% at 2 μm.

3. GaSe saturable absorber for SQS operation

With all the mirrors in the laser cavity aligned, CW operation could be achieved. And then slightly adjust the input coupler or the output coupler, leading to an unstable SQS operation. The spectral widths of the CW and self-Q-switched operation were 2.8 nm and 2.5 nm. Fig. 2 shows the pulse train of the SQS Tm:YAG laser with OC of 10%. Fig. 2(a) shows the multiple pulse trains, and Fig. 2(b) shows one typical pulse profile. Fig. 3 shows the pulse train of the SQS Tm:YAG laser with OC of 15%. Fig. 3(a) shows the multiple pulse trains, and Fig. 3(b) shows one typical pulse profile. When the SQS operation was occurred, the power jitter was less than 2.5%. Therefore, the SQS operation was

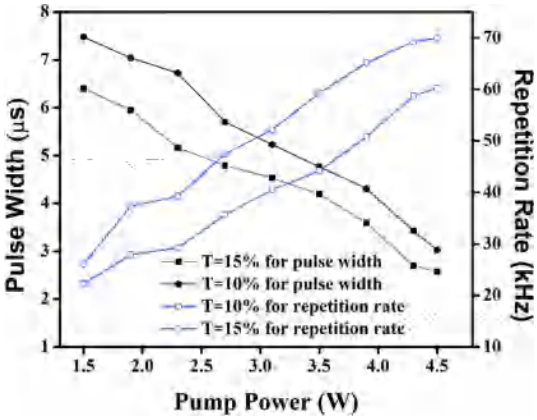

Fig. 5. The relationship between different laser condition and the pump power in SQS operation.

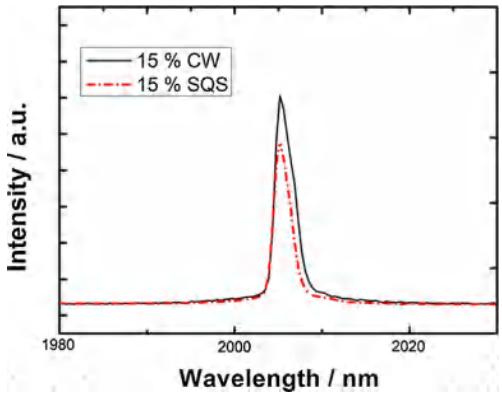

Fig. 6. Spectrum of the CW and SQS operations with OC of 15%.

Table 1
The SQS operation in Tm:YAG crystal with other Tm-doped crystals.

Crystal	Output power	Pulse width	Mechanism	Ref
Tm:YLF	0.61 W	1.5 μs	Saturable GSRA effect	[8]
Tm:$YAlO_3$	–	12.5 μs	Nonlinear dynamics with chaotics	[20]
Tm:YAP	1.68 W	1.64 μs	Time-depended lens	[21]
Tm:YAG	0.87 W	2.57 μs	Time-depended lens	[Paper]

quite stable. The SQS operation in Tm:YAG crystal may cause by the thermal lensing effect which lead to the changes of refractive index with the laser intensity. Finally, a time-dependent lens had be formed inside the crystal and lead to the nonlinear loss mechanism [18].

Fig. 4 shows the output power versus the incident pump power under CW and SQS operations. The ● line showed the relationship between the incident pump power and the output power of the CW operation with OC of 10%. The pump power increased from 1.4 W to 4.4 W, and the output power increased from 0.02 W to 1.03 W. The ○ line showed the relationship between the incident pump power and the output power of the CW operation with OC of 15%. The pump power increased from 1.6 W to 4.4 W, and the output power increased from 0.11 W to 1.52 W. With the pump power of 4.4 W, we got two sets of data: (1) the optical conversion efficiency of the CW operation with OC of 10% was 23.41%; (2) the optical conversion efficiency of the CW operation with OC of 15% was 34.55%. The ▼ line showed the relationship between the incident pump power and the output power of the SQS operation with OC of 10%. The pump power increased from 2 W to 4.4 W, and the output power increased from 0.066 W to 0.55 W. The △ line showed the relationship between the incident pump power

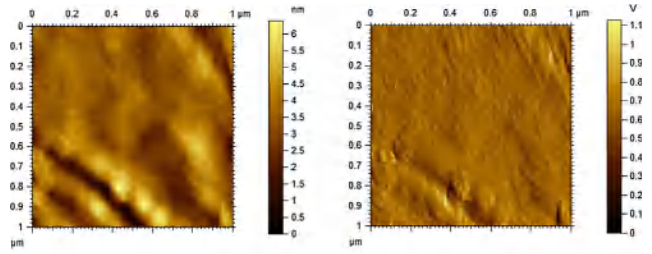

(a) AFM images of intentionally scratched samples

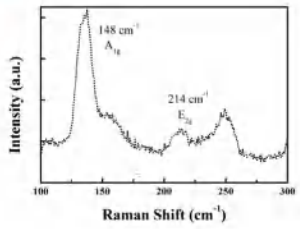

(b) reflecting Raman spectrum of few-layer GaSe SA

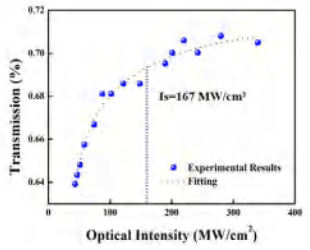

(c) nonlinear absorption property of GaSe SA

Fig. 7. Characterization of GaSe SA.

and the output power of the SQS operation with OC of 15%. The pump power increased from 2.2 W to 4.4 W, and the output power increased from 0.069 W to 0.87 W. With the pump power of 4.4 W, we got two sets of data: (1) the optical conversion efficiency of the SQS operation with OC of 10% was 12.50%; (2) the optical conversion efficiency of the SQS operation with OC of 15% was 19.77%.

Fig. 5 shows the relationship between different laser conditions (the pulse width and repetition rate) and the pump power in SQS operation. The ■ line showed the relationship between the pump power and the pulse width with OC of 15%. The pump power increased from 1.5 W to 4.5 W, and the pulse width decreased from 6.40 μs to 2.57 μs. The ● line showed the relationship between the pump power and the pulse width with OC of 10%. The pump power increased from 1.5 W to 4.5 W, and the pulse width decreased from 7.48 μs to 3.03 μs. The □ line showed the relationship between the pump power and the repetition rate with OC of 10%. The pump power increased from 1.5 W to 4.5 W, and the repetition rate increased from 22.28 kHz to 60.24 kHz. The ○ line showed the relationship between the pump power and the repetition rate with OC of 15%. The pump power increased from 1.5 W to 4.5 W, and the repetition rate increased from 26.13 kHz to 69.94 kHz.

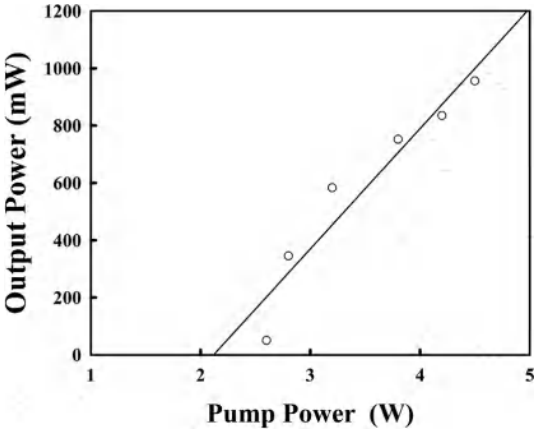

Fig. 9. Output power versus pump power under passively Q-switched operations with OC of 10%.

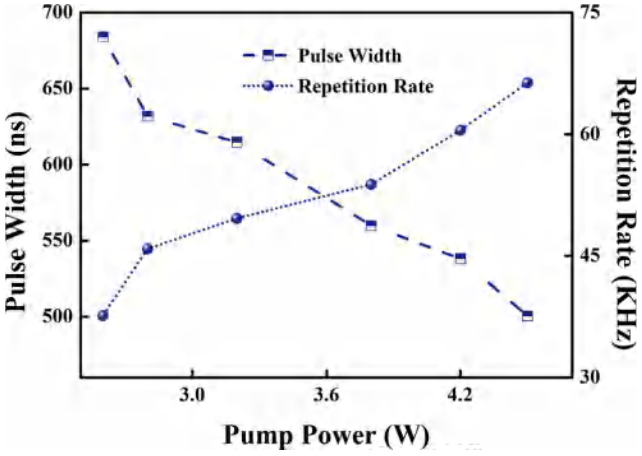

Fig. 10. Functions of the pulse width, repetition rate and the pump power.

Fig. 6 shows the spectrum of the CW and SQS operations with OC of 15%. The central wavelength of the Tm:YAG laser was 2006 nm. The output spectrum was consistent with the peak fluorescence wavelength of the Tm:YAG crystal.

The SQS mechanism in Tm-doped crystal could be explained by the nonlinear dynamics time-depended lens inside the crystal [18,20–21]. The changing refractive index caused by thermal lensing effect inside the Tm:YAG crystal leading to the time-dependent lens. In Table 1, we have compared the SQS operation in Tm:YAG crystal with other Tm-doped crystals.

4. GaSe saturable absorber for passively Q-switched operation

The laminate of GaSe nanosheets was fabricated by liquid

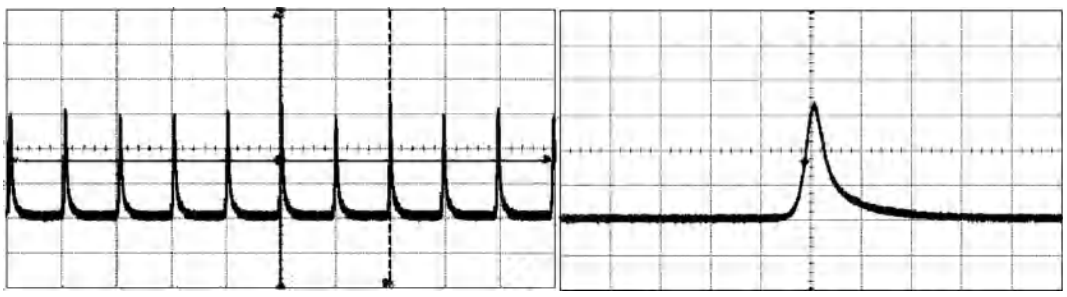

Fig. 8. (a) The multiple pulse trains (20 μs/div), (b) one typical pulse profile (500 ns/div).

exfoliation method. Firstly, added 0.1 g GaSe powder (purity of 99.9%) into 50 ml mixture solution (alcohol and water of 3:7), ultrasound the mixture solution for 6 h. Secondly, centrifuged the solution for 30 min at speed of 2500 rpm, then stirred its supernatant with 50 ml PVA (4 wt %) for 7 h. Then, transferred the mixture to quartz chip and put the quartz chip in the dryer for 24 h at 25 ℃. Finally, the GaSe saturable absorber was ready.

The nonlinear absorption property T could be expressed as follows:

$$T = 1 - T_1 - T_2 - \exp(-I/I_s)$$

where, T_1 is unsaturated absorbance, T_2 is modulation depth, I and I_s are laser intensity and laser saturation intensity.

Fig. 7 shows the characterization of GaSe SA. Fig. 7(a) shows the AFM images of intentionally scratched samples. The step height was 5.8 nm, and this sample has 6 layers. Raman spectroscopy is a non-destructive characterization of GaSe SA. Fig. 7(b) shows the reflecting Raman spectrum of few-layer GaSe SA by using a 532 nm laser at room temperature. The in-plane vibration peak E^1_{2g} and out of-plane vibration peak A^1_{2g} belonged to GaSe material [19]. In Fig. 7(c), the nonlinear absorption property of GaSe SA is demonstrated using a femtosecond laser with 780 fs pulses at 1040 nm. The experimental results indicated that the saturation intensity and modulation depth were 167 MW/cm^2 and 6.7%, respectively.

Firstly, recovered all the mirrors aligned and found the CW operation. Then, inserted GaSe SA into the laser cavity, the passively Q-switched operation could be obtained. Fig. 8 shows the pulse train of passively Q-switched Tm:YAG laser with OC of 10%. Fig. 8(a) shows the multiple pulse trains, and Fig. 8(b) shows one typical pulse profile.

Fig. 9 shows the output power versus pump power under passively Q-switched operations with OC of 10%. The pump power increased from 2.6 W to 4.4 W, and the output power increased from 0.05 W to 0.9 W. The slope efficiency of the passively Q-switched operation was 20%. Fig. 10 shows the functions of pulse width, repetition rate and pump power. The dash line showed the relationship between pump power and pulse width with OC of 10%. The dot line showed the relationship between pump power and pulse width with OC of 10%. The pump power increased from 2.6 W to 4.5 W, the pulse width decreased from 684 ns to 500 ns, and the repetition rate increased from 32.6 kHz to 66.8 kHz.

5. Conclusion

In this paper, a fiber-coupled diode-pump SQS Tm:YAG laser at 2006 nm was designed. With the pump power of 4.4 W, we got two sets of data: (1) the optical conversion efficiency of the SQS operation with OC of 10% was 12.50%; (2) the optical conversion efficiency of the SQS operation with OC of 15% was 19.77%. In addition, GaSe SA was fabricated and employed as a SA for passively Q-switched Tm:YAG laser. The passively Q-switched operation with 10% OC was demonstrated. The repetition rate of 66.8 kHz, narrowest pulse width of 500 ns were obtained. In summary, GaSe is a good 2D SA material in wide-wavelength range.

Declaration of Competing Interest

The authors declared that there is no conflict of interest.

References

[1] D. Welford, Passively Q-switched lasers, Circuits Dev. Mag. IEEE 19 (4) (2003) 31–36.
[2] I. Freund, Self-Q-switching in ruby lasers, Appl. Phys. Lett. 12 (11) (1968) 388–390.
[3] J.L. Xu, Y.X. Ji, Y.Q. Wang, et al., Self-Q-switched, orthogonally polarized, dual-wavelength laser using long-lifetime Yb^{3+} crystal as both gain medium and saturable absorber, Optics Express 22 (6) (2014) 6577–6585.
[4] S.C. Bai, J. Dong, GTR-KTP enhanced stable intracavity frequency doubled Cr, Nd:YAG/KTP miniature green laser, IEEE Photon. Technol. Lett. 25 (9) (2013) 848–850.
[5] J. Dong, Y. He, X. Zhou, et al., Highly efficient, versatile, self-Q-switched, high-repetition-rate microchip laser generating Ince-Gaussian modes for optical trapping, Quant. Electron. 46 (3) (2016) 218–222.
[6] J. Liu, X. Fan, J. Liu, et al., Mid-infrared self-Q-switched Er, Pr:CaF_2 diode-pumped laser, Opt. Lett. 41 (20) (2016) 4660–4663.
[7] H.S. He, Z. Chen, H.B. Li, et al., Low-threshold, nanosecond, high-repetition-rate vortex pulses with controllable helicity generated in Cr, Nd:YAG self-Q-switched microchip laser, Laser Phys. 28 (5) (2018) 055802.
[8] B. Zhang, L. Li, C.J. He, et al., Compact self-Q-switched Tm:YLF laser at 1.91μm, Opti. Laser Technol. 100 (2018) 103–108.
[9] Q. Song, G. Wang, B. Zhang, et al., Dual-wavelength self-Q-switched Nd:GYSGG laser, J. Modern Opt. 62 (19) (2015) 1655.
[10] Q. Song, G. Wang, B. Zhang, W. Wang, M. Wang, Q. Zhang, G. Sun, Y. Bo, Q. Peng, Diode-pumped passively dual-wavelength Q-switched Nd: GYSGG laser using graphene oxide as the saturable absorber, Appl. Opt. 54 (10) (2015) 2688–2692.
[11] Q. Song, Z. Wu, P. Ma, et al., TiS2, MoS2, WS2/Sb2Te3 mixed nanosheets saturable absorber for dual-wavelength passively Q-switched Nd:GYSGG Laser, Infrared Phys. Technol. 92 (2018) 1–5.
[12] H. Ahmad, M.R.K. Soltanian, C.H. Pua, M. Alimadad, S.W. Harun, Photonic crystal fiber based dual-wavelength Q-switched fiber laser using graphene oxide as a saturable absorber, Appl. Opt. 53 (2014) 3581.
[13] D. Mao, X.Y. She, B.B. Du, D.X. Yang, W.D. Zhang, K. Song, X.Q. Cui, B.Q. Jiang, T. Peng, J.L. Zhao, Erbium-doped fiber laser passively mode locked with few-layer WSe_2/$MoSe_2$ nanosheets, Sci. Rep.-UK 6 (2016) 23583.
[14] M. Yüksek, A. Elmali, M. Karabulut, et al., Switching from negative to positive nonlinear absorption in p type 0.5 at% Sn doped GaSe semiconductor crystal, Opt. Mater. 31 (11) (2009) 1663–1666.
[15] U. Kürüm, M. Yüksek, H.G. Yaglioglu, et al., The effect of thickness and/or doping on the nonlinear and saturable absorption behaviors in amorphous GaSe thin films, J. Appl. Phys. 108 (6) (2010) 063102.
[16] H. Ahmad, S.N. Aidit, S.I. Ooi, et al., Tunable passively Q-switched ytterbium-doped fiber laser with mechanically exfoliated GaSe saturable absorber, Chin. Opt. Lett. 16 (2) (2018) 020014.
[17] H. Huang, P. Wang, Y. Gao, et al., Highly sensitive phototransistor based on GaSe nanosheets, Appl. Phys. Lett. 107 (14) (2015) 143112.
[18] Q. Song, G. Wang, B. Zhang, et al., Dual-wavelength self-Q-switched Nd: GYSGG laser, J. Modern Opt. 62 (19) (2015) 1655–1659.
[19] Xufan Li, Ming-Wei Lin, Junhao Lin, Bing Huang, Alexander A. Puretzky, Cheng Ma, Wang Kai, Wu Zhou, Two-dimensional GaSe/$MoSe_2$ misfit bilayer heterojunctions by van der Waals epitaxy, Sci. Adv. 2 (4) (2016) e1501882.
[20] K.S. Wu, O. Henderson-Sapir, P.J. Veitch, M. Hamilton, J. Munch, D.J. Ottaway, Self-pulsing in Tm-doped $YAlO_3$ lasers: excited-state absorption and chaos, Phys. Rev. A 91 (4) (2015) 043819.
[21] W. Cai, J. Liu, C. Li, H.T. Zhu, P.G. Ge, L.H. Zheng, L.B. Su, J. Xu, Compact self-Q-switched laser near 2 μm, Opt. Commun. 334 (2015) 287–289.